

X-RAY AND ULTRAVIOLET PHOTOEMISSION  
OF POLYMERIC SULFUR NITRIDE (SN)<sub>x</sub>

P. MENGEL

Institut für angewandte Physik, Universität Karlsruhe, FRG

I.B. ORTENBURGER, W.E. RUDGE, and P.M. GRANT

IBM Research Laboratory, San Jose, California 96193, USA

ABSTRACT

We have determined, both experimentally and theoretically, the one-electron density of states surrounding the Fermi level in polymeric sulfur nitride, (SN)<sub>x</sub>. The experimental measurements were performed using X-ray and ultraviolet photoemission spectroscopy (XPS and UPS), while the theoretical studies employed calculations based on OPW and pseudopotential band structures of (SN)<sub>x</sub>. The XPS measurements included observations of N and S core level shifts which yielded values for the number of charged-transferred electrons of about 0.4. This is compared with our recent XPS data on a related compound, Se<sub>4</sub>N<sub>4</sub>, yielding a charge transfer of 0.3 e only. One of the major observations from both XPS and UPS was that of low photoemissive yields near the Fermi level. Our calculations of the photoemissive response tensor,  $D_{\mu\nu}(E, h\nu)$ , show that this low yield near  $E_F$  is primarily a result of dipole matrix element energy dependence.

In order to gain information on the electronic structure of polymer sulfur nitride,  $(\text{SN})_x$ , we investigated the photoemission properties of this interesting material. The measurements were obtained on nonoriented  $(\text{SN})_x$  films using x-ray and variable ultraviolet photoemission spectroscopy (XPS and UPS) (1), (2). Table 1 shows the nitrogen and sulfur core levels in  $(\text{SN})_x$  and in neutral elements. Also included in table 1 is the nitrogen core level energy of  $\text{Se}_4\text{N}_4$  from our current XPS measurements on this material (3). Siegbahn (4) has found an experimental relationship between the binding energy and net charge as determined by the chemical shifts of the S(2p) and N(1s) lines in several nitrogen - and sulfur - containing compounds. Applying his criteria to our N(1s) core level energies, we obtain a net charge transfer figure in  $(\text{SN})_x$  and  $\text{Se}_4\text{N}_4$ . The results are shown in table 2 together with results of charge transfer in  $(\text{SN})_x$  and  $\text{S}_4\text{N}_4$  taken from XPS data of Salaneck et al (5).

Comparing the results of the  $\text{Se}_4\text{N}_4$  and  $\text{S}_4\text{N}_4$  structures, we note that only half as much charge is transferred in the SeN bond. Salahub and Messmer (6) have calculated a charge transfer of 0.5 e for  $(\text{SN})_x$  by the self consistent-field  $X\alpha$  standing wave method, resulting in a large dipolemoment for the SN bond. Further it is shown, that this dipolemoment is the determining factor for the square planar geometry of  $\text{S}_2\text{N}_2$ , from which by thermal excitation the polymerization process is very likely to occur. In the important question of analogs one would expect that substitutions for S and N such that a larger difference in electronegativity results are more favorable. One realistic possibility here is believed to be a replacement of S by Se. However, the decrease of the charge transfer in SeN as determined from our XPS data indicates a much less stable hypothetical  $\text{Se}_2\text{N}_2$  structure in a  $\text{S}_2\text{N}_2$  geometry. This may explain why so far all attempts by the chemists to prepare  $\text{Se}_2\text{N}_2$  and  $(\text{SeN})_x$  analogs have failed.

The XPS spectrum for the valence band region of  $(SN)_x$  is shown in Fig.1. In the lower half of the figure the experimental results are directly compared with two theoretically derived single-particle density of states (DOS). A one-dimensional tight-binding extended Hückel (1DTB) computation has been published by Thomas and Parry (7) and a three dimensional OPW (3DOPW) calculation was done by Rudge and Grant (8). Both theoretical DOS show good overall qualitative agreement with the experimental data and in addition the 3DOPW DOS gives good quantitative agreement in peak energy positions and relative peak intensity ratios. The 3DOPW DOS presented here is based on the older Lyon or Boudeulle crystal structure. When using the newer crystal structure with less S-S coupling, referred to as Penn structure, the theoretical DOS remains remarkably unchanged. The only difference is a shift of peak 1 by 0.8 eV to lower energies. It is shown in reference (8) that this shift arises from a displacement of certain intrachain bands and none of the DOS structure appears directly related to interchain bands. Thus, one cannot expect the XPS data to be sensitive to interchain coupling, which explains the overall good agreement with the pure 1DTB DOS.

A low density of states at the Fermi level was found in the experiment. A simple area calibration to 44 electrons yields a value of 0.04 states/(eV x spin x molecule). This number should be considered as a crude estimate only, due to different photoionization cross section of sulfur and nitrogen orbitals and other experimental errors.

In the UPS measurements we were able to prepare the  $(SN)_x$  films inside of the UHV chamber. X-ray analysis and electron reflection patterns show the  $(\bar{1}02)$  plane of  $(SN)_x$  to lie parallel to the substrate plane in a textured orientation. A family of electron distribution curves (EDCs) for photon energies of  $7.6 \text{ eV} \leq h\nu \leq 11.1 \text{ eV}$  is shown in Fig.2. The EDCs

do not show much structure but one would not expect that from the XPS data and the calculated DOS. We see well resolved now the first peak at 1 eV below  $E_F$ , also a peak at 4.5 eV and a further structure at 2.5 eV. The most surprising result is the very low electron yield at the Fermi level, which in fact lies more or less within the sensitivity limitation of the spectrometer.

In order to relate the experimental structure to the density of occupied states and to clarify the low electron yield at the Fermi level, an extended calculation of the photoemissive response tensor  $D_{\mu\nu}(E, h\nu)$  was undertaken based on pseudopotential band structure calculation (9). In Fig.3 we compare experimental and calculated EDCs for some values of exciting photon energy. We like to point out that we also accounted for the observed textured film structure. This was achieved by applying an arbitrary rotation on the  $D_{\mu\nu}(E, h\nu)$  tensor around an axis perpendicular to the sample surface and averaging over all angles.

For low photon energies we find a reasonable agreement between theory and experiment. The entire experimental structure is revealed in the theoretical data. We used here the Penn crystal structure - which we believe is proved to be the more accurate one - but that leads to a disagreement in energy position of about 0.6 eV for the first peak below  $E_F$ . A better agreement for this peak was obtained when using the Lyon crystal structure. No agreement between experimental and calculated EDCs is found for photon energies greater 10 eV as shown in Fig.3 for  $h\nu = 11.1$  eV. We think it is unreasonable to assume, that the pseudopotential method is sufficiently accurate to determine the conduction bands far above the Fermi level. Of overriding importance is the

fact, that the calculated EDCs show the same low photoemissive yield at  $E_F$ . To investigate the reasons for this low electron contribution at  $E_F$ , we calculated the energy dependence of the average matrixelement (9). This is shown in the lower half of Fig. 4 for one particular photon energy of  $h\nu = 7.9$  eV. In the upper half of the figure we computed the distribution curve based on a simple joint density model with constant matrixelement assumption for the same photon energy.

The explanation is obvious. In the joint density model we obtain an electron yield of 0.03 states/(eV x spin x molecule) at  $E_F$  comparable with the XPS data. However, the matrixelement dependence shows that the transition probability at  $E_F$  is only 1/5 of the average value ( $\equiv 1$ ).

The product of both matrixelement energy function and joint density of states leads then directly to a neglecting small electron yield at the Fermi level in excellent agreement with the experimental results.

We note that no explanations based on relaxation or localization effects are used to explain this low photoemissive yield at  $E_F$ . Thus, as far as the analysis of photoemission data in general is concerned, a constant matrixelement assumption can easily lead to wrong conclusions about the importance of such effects.

Table 1: XPS determined core level energies of sulfur and nitrogen in  $(SN)_x$ , in  $Se_4N_4$  and in neutral elements.

Element	Level	Binding Energy (eV) in $(SN)_x$	Binding Energy (eV) in $Se_4N_4$	Binding Energy (eV) for neutral Elements
N	$1S_{1/2}$	- 397.3	- 398	- 399
S	$2S_{1/2}$	- 228.5		- 229
	$2P_{3/2}$	- 163.5		- 162
	$2P_{1/2}$	- 164.5		- 163
	$2P^a)$	- 164.5		

a) After long exposure (> 4h) to air or the XPS X-ray beam.

Table 2: Charge transfer values  $\delta$  for  $S^{+\delta}N^{-\delta}$  and  $Se^{+\delta}N^{-\delta}$  in  $(SN)_x$ ,  $S_4N_4$  and  $Se_4N_4$  from XPS data.

Structure	Reference	Charge Transfer $\delta(e)$
$(SN)_x$	this work	0.42
	Salaneck et al 5	0.5
$S_4N_4$	Salaneck et al 5	0.6
$Se_4N_4$	this work	0.29

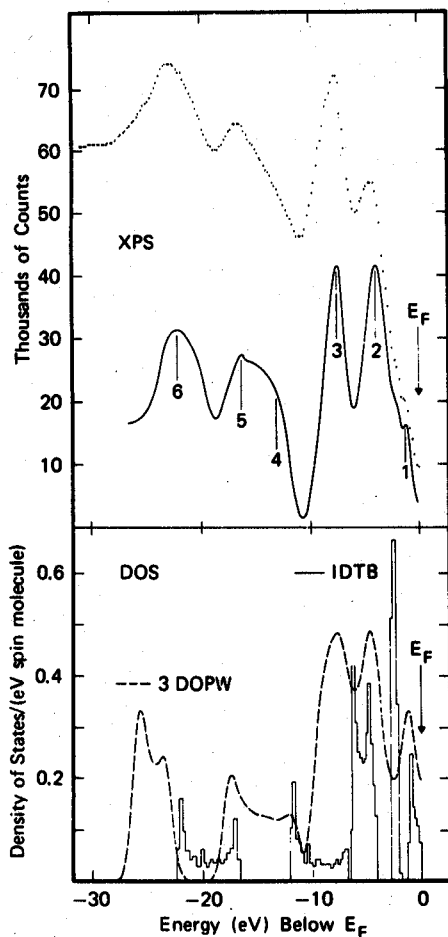


Figure 1: Top: X-ray photoemissions spectrum, raw data (dotted line) and background corrected data (solid line). Bottom: One-electron valenceband density of states for a one-dimensional planar chain (IDTB, solid line), and for a three-dimensional OPW calculation based on the Lyon crystal structure (3DOPW, broken line). The ordinate scale refers only to the OPW result which was obtained using an 0.25 eV Gaussian broadening function.

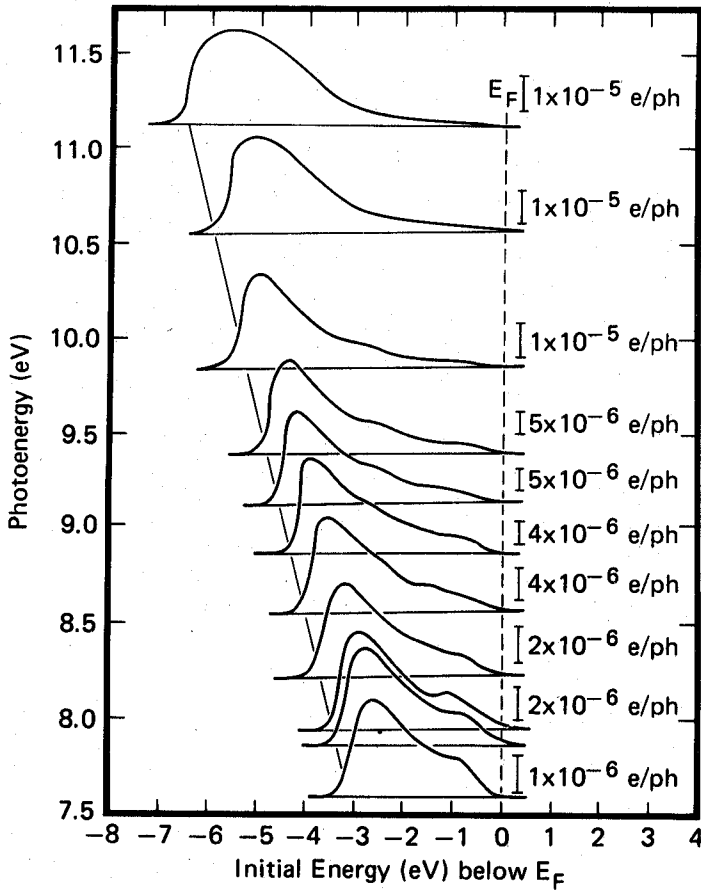


Figure 2: A family of EDCs for  $7.6 \text{ eV} \leq h\nu \leq 11.1 \text{ eV}$  from an about  $1 \mu$  thick  $(\text{SN})_x$  film. Each curve is normalized to its maximum. In absolute values the quantum yield for the highest photon energy  $h\nu = 11.1 \text{ eV}$  is more than a factor of 10 greater than for the lowest photon energy. On a more sensitive scale the distribution curve for  $h\nu = 11.1 \text{ eV}$  reveals all the structure shown in EDCs for the lower photon energies. The diagonal line marks zero kinetic energy.



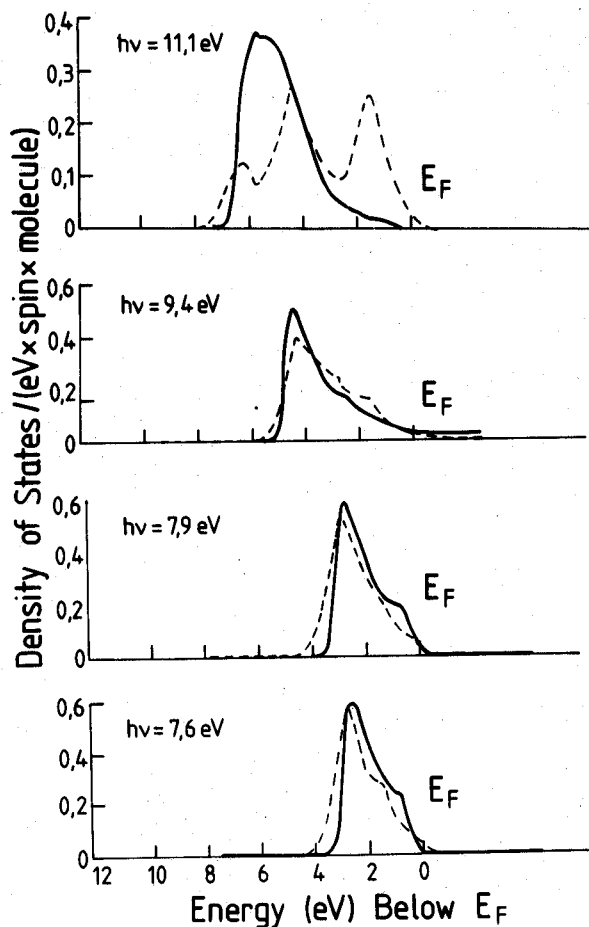


Figure 3: A comparison between calculated (broken line) and experimental (solid line) EDCs for  $h\nu = 7.6, 7.9, 9.4$  and  $11.1$  eV. All experimental and theoretical curves are normalized to the total quantum yield.

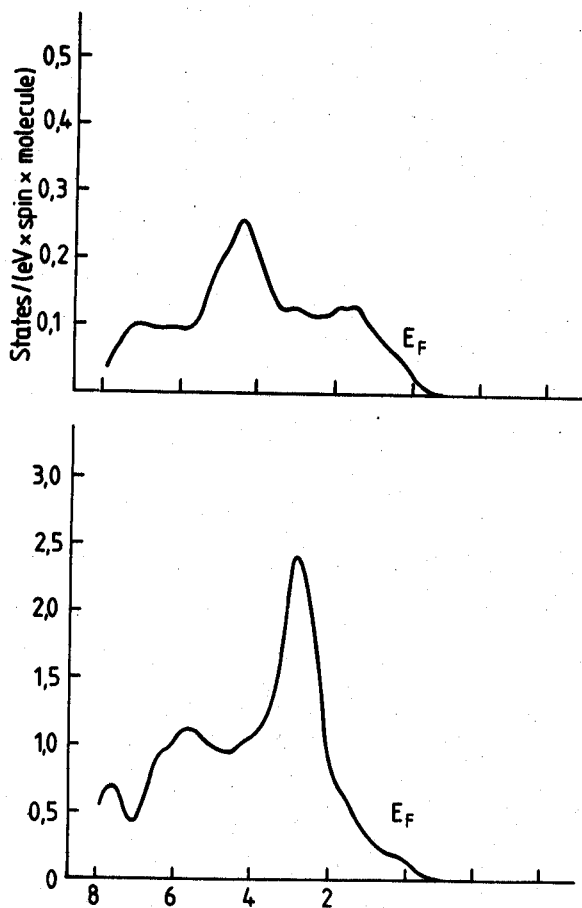


Figure 4: Top: EDC for  $h\nu = 7.9$  eV based on simple joint density model.  
 Bottom: Average dipole matrix element function  $M(E, h\nu)$  for the same photon energy.

## REFERENCES

- 1) P.MENGEL, P.M. GRANT. W.E. RUDGE, B.H.SCHECHTMAN  
and D.W. RICE  
Phys.Rev.Lett. 35, 1803 (1975)
- 2) P.MENGEL, I.B.ORTENBURGER and P.M.GRANT  
Submitted to phys.rev.
- 3) P.MENGEL, C.BRULET and G.B.STREET  
to be published
- 4) K.SIEGBAHN, C.NORDLING, A.FAHLMAN, R.NORDBERG, K.HAMRIN,  
J.HEDMAN, G.JOHANSSON, T.BERGMARK, S.E.KARLSSON, I.LINDGREN  
and B.LINDBERG,  
in ESCA; Atomic, Molecular and Solid State  
Structure Studies by means of Electronic  
Spectroscopy (Almquist and Wiksells, Uppsala, Sweden,  
(1967)
- 5) W.R.Salaneck, J.W.p Lin, and A.J.EPSTEIN  
Phys.Rev.B 13, 5574 (1976)
- 6) D.R.SALAHUB and R.P.MESSMER  
submitted to J.ChemPhys.
- 7) D.E.PARRY and J.M.THOMAS  
J.Phys.C: Solid State Phys. 8, L 45 (1975)
- 8) W.E.RUDGE and P.M.GRANT  
Phys.Rev.Lett. 35, 1799 (1975)
- 9) For details see ref. 2 and P.M.Grant, W.E.RUDGE  
and I.B.ORTENBURGER this volume.